

IV. Conclusions

All of the fuels tested in this program changed in octane rating as the pressure of the altitude chamber was decreased. In general, the fuels that were the most sensitive to altitude changes were those with the highest sensitivity to engine severity, as defined by the differences between their Motor Method and Research Method ratings. This is to be expected, as the higher compression ratios used at lower chamber pressures increase the engine severity by raising the compression temperatures.

It has been shown that decreased inlet temperature and decreased speed shift altitude ratings by the Motor Method toward their sea-level values, but at different rates for various fuels. Although the effects of spark advance on this method were not investigated, a change in this factor might prove advantageous. Larger carburetor venturis have proved useful, and permit ratings to be maintained at about their sea-level values up to altitudes to 3,000 to 4,000 ft. It is possible that the Motor Method ratings are capable of being equalized throughout the altitude range by use of a suitable combination of changed conditions.

The Research Method, on the other hand, does not lend itself well to modifications of this type. The spark advance is already nearly the optimum, inlet temperature is at about the minimum that will assure adequate vaporization of the fuel, the volumetric efficiency is improved very little by use of a larger venturi, and the engine speed is already very low.

It appears, therefore, that the surest way of making the engine severity equal to that at sea level, regardless of the altitude, is to supercharge the inlet and throttle the exhaust, thereby simulating sea-level conditions. For this purpose, a small single-stage centrifugal compressor would probably suffice. The

air would enter the blower through a standard humidity-controlling ice tower, and thence through the standard air heater to a pressurized carburetor. It is possible that an after-cooler may also be necessary to keep the inlet temperature below 125° F in the Research Method at the lower chamber pressures.

This investigation was carried out in cooperation with the Octane Correlation Advisory Committee of the Division of Refining of the American Petroleum Institute. Members of this committee are: Bruno R. Siegel, chairman, Frank C. Burk, Carl E. Habermann, J. E. Taylor; associate members are Harold M. Trimble, H. R. Stacey, John M. Snell, Afton D. Puckett, and Hudson W. Kellogg. Appreciation is expressed to the committee members for planning the scope of the work and their expert advice in carrying it out. Credit is also due the following for their work in operating the engines and altitude equipment: W. C. Lacey, Myron C. Wolfe, James O. Chase, H. B. Dickerson, J. M. Mealing, L. J. Wilson, H. S. Simmons, Fred W. Ramin, George J. Miner, Edwin H. Rich, Richard M. David, James A. Walker, Milford Barnes, Thomas W. Mears, and Mrs. Cecil S. Dussinger.

V. References

- [1] W. M. Holaday and G. T. Moore, Effect of altitude on octane number determination, presented at SAE Annual Meeting, January 1937.
- [2] D. B. Brooks, Effect of altitude on knock rating in CFR engines, J. Research NBS **28**, 713 (1942) RP1475.
- [3] ASTM manual of engine test methods for rating fuels and 1948 appendix (American Society for Testing Materials, 1916 Race Street, Philadelphia 3, Pa.).
- [4] O. C. Bridgeman, Equilibrium volatility of motor fuels from the standpoint of their use in internal combustion engines, J. Research NBS **13**, 53 (1934) RP694.

WASHINGTON, April 10, 1950.

Creep of High-Purity Copper

By William D. Jenkins and Thomas G. Digges

Creep tests were made at 110°, 250°, and 300° F on annealed oxygen-free high-conductivity copper. The rate of loading to the ultimate had a significant effect on the amount of plastic extension and thereby affected the creep behavior. The strain rate during the so-called second stage of approximately constant rate was not constant but varied in a cyclic manner. A less-pronounced cyclic variation was also evident in both the first and third stages. The beginning of the third stage was often accompanied by microcracking, but in other tests this stage was initiated without the presence of such cracks. The parent grains were fragmented during creep, and strain markings were observed in all specimens carried to complete fracture.

I. Introduction

Creep tests in tension were made on annealed oxygen-free high-conductivity copper as a part of a continuing investigation at this Bureau on the creep

of metals and alloys. Additional tests at elevated and subzero temperatures on this copper and other materials are in progress. In a previous paper [1]¹ it was shown that the flow, ultimate and fracture

¹ Figures in brackets indicate the literature references at the end of this paper.

stresses, and ductility increased with a decrease in test temperature and with an increase in strain rate of another lot of oxygen-free high-conductivity copper initially cold-rolled 75-percent reduction in area.

Parker and Riisness [2] reported that the creep strength at 200° C of annealed oxygen-free high-conductivity copper was independent of the grain size. Parker [3] also determined the stress-rupture properties at 200° C of this type of copper initially in the conditions as (1) annealed, (2) cooled in air, and (3) quenched in water from 850° C. The strength and ductility of the quenched specimens were appreciably lower than those of the specimens as annealed or as cooled in air. A linear relation was shown in a log-log plot of the experimental values of the stress versus the time to rupture for both the annealed and air-cooled conditions, but there were points at which changes occurred in the slope of the curve for the initially quenched specimens. Some recrystallization occurred in specimens, which were cold-rolled from 1.0 to 0.1 in. in thickness, after heating at 200° C for 20 hr.

Davis [4] made a study of the creep and relaxation (constant deformation) at temperatures up to 235° C of oxygen-free copper initially extended 8 percent in tension, and he attempted to correlate the results of the two different types of tests by using various theories of plastic deformation. At 235° C, the creep (extension-time) curves tended to become straight after about 400 hr, but at 165° C they did not become straight until after about 1,200 hr; at 30° C, the curves had not reached a constant slope after 3,500 hr. The stresses used in these creep tests ranged from 12,000 to 16,000 psi at 30° C, 4,000 to 10,000 psi at 165° C, and 2,500 to 7,000 psi at 235° C. The logarithms of minimum creep rates for all the tests, except those at 30° C, were plotted against the stress, and straight lines were drawn to fit these data (semilog plot). He concluded that the hyperbolic-sine relation between the minimum creep rate and stress fitted the test data very well. No accurate theory existed by which the shape of the relaxation curve could be predicted from data observed in creep tests when the temperatures were within the range covered in these tests. The strain rate in the latter stages of a relaxation test was slower than the minimum creep rate for the corresponding stress.

Burghoff and Blank [5] presented data on creep at 300°, 400°, and 500° F of four types of wrought copper and several copper alloys initially as annealed and as cold-drawn. Usually, their creep tests did not progress beyond the first stage (that of decreasing rate under constant load) within a period of about 6,000 hr; the values reported for creep rate were those obtained in the latter part of the test. A linear relationship was shown in a log-log plot of the experimental values of stress versus strain rate for oxygen-free copper (99.98 percent copper) initially both as annealed (0.025-mm grain diameter) and as

cold-drawn 84 percent. The cold-drawn specimens became about half recrystallized during the course of the tests at 300° F and completely recrystallized at 400° F shortly after the creep load was applied.

Schwoppe, Smith, and Jackson [6] recently investigated the effect of cold work on the short-time creep strength in tension and compression at 570° F and on the long-time creep strength in tension at lower temperatures (200° to 300° F) of several types of commercial copper, including the oxygen-free high-conductivity grade. They reported that cold work increases the creep strength of copper, but its beneficial effect is lost at temperatures where recrystallization was rapid. The trends in the short-time creep tests were also evident in the longer time creep tests. A linear relation was shown in plots of stress versus log of strain rate of the experimental values for both the short- and long-time tests.

II. Material and Testing Procedures

All specimens were cut from a bright annealed 1/8-in. round bar of oxygen-free high-conductivity copper (OFHC) containing 99.99+ percent of copper as determined by chemical analysis. The arc spectrum of the copper was examined for the sensitive lines of Ag, Al, B, Be, Co, Fe, In, Ir, Mg, Mo, Na, Ni, Pb, Sb, Si, Sn, Ti, V, and Zn. The lines for Ag, Al, Mg, and Si were identified, and there was some indication of the presence of Fe, Ni, and Pb.

Some properties at room temperature of the annealed copper were as follows:

Average grain diameter, mm.....	0.025
Average hardness, Rockwell F.....	34
Tensile strength, 1,000 psi.....	31.9
Yield strength, (0.2 percent offset) 1,000 psi.....	12.2
Elongation in 2 in., percent at maximum load.....	39
Elongation in 2 in., percent at fracture.....	51
Reduction of area, percent at maximum load.....	28
Reduction of area, percent at fracture.....	88

The creep tests were made on specimens having a 0.505-in. gage diameter and a gage length of 2 in.; all specimens were prepared from the same bar. The tests were carried out in a noncontrolled atmosphere (air) at temperatures of 110°, 250°, and 300° F. The temperatures of the creep furnaces were controlled within the range of about ±1 deg F of the desired temperature (temperature differences within the gage length of the test specimen were less than 3 deg F), and the probable error of extension measurements was less than 0.00002 in. The specimens were held for a minimum of 48 hr at temperature before loading, and the rate of loading of each specimen to the selected ultimate² stress was accurately controlled. Each creep test was made at a constant load, which was maintained for the complete test. A rate of loading of 3,200 psi/hr (3,200 psi applied at 1-hr intervals) was selected as a

² The terms "ultimate stress" are used to designate the selected stress applied to a specimen for testing in creep at a constant load. The value for ultimate stress is obtained by dividing the load by the original area of the specimen.

"standard," and this rate was used in all tests except those in which the rate of loading was varied to determine its effect on creep behavior. When the ultimate stress (nominal)³ was not divisible by 3,200, the remainder was added as the final step.

The equipment used for creep testing is essentially the same as that used and described in previous investigations [7]; some improvements have been made, especially in temperature controllers, measuring microscopes, and method of attaching the strips to specimens for measuring the extension.

Rockwell F hardness (60-kg load, 1/16-in.-diameter

³ The nominal stress is defined as the stress obtained by dividing the current load by the original area of the specimen. The true stress is defined as the stress obtained by dividing the current load by the current minimum area of the specimen.

ball) measurements were made on the bar as annealed and on selected specimens after testing either in creep or in normal tension at room temperature. Two flats 180° apart were prepared parallel to the longitudinal axis of the specimens tested to fracture in tension, and the Rockwell readings were made at room temperature on various points along the center line of these flats. The diameters of the specimens at the points of indentation were accurately determined by means of a measuring microscope. Thus, the hardness values could be correlated with the degree of plastic deformation.

Usual procedures were followed in preparing specimens by mechanical methods for metallography and in carrying out the metallographic examinations.

TABLE 1. Summary of conditions used and results of creep and tension tests on high-purity copper initially as bright annealed

Thermal mechanical history	Temperature	Ultimate stress	Loading schedule	Creep rate	Time	Plastic extension	Beginning of third stage			End of test				Remarks
							Time	Plastic extension	True stress	Time	Plastic extension	Reduction of area	True stress	
Initially as annealed	80	31.9		60,000			0.7	39.	44.0	1.25	51.0	88	140.0	Tested to fracture.
Do.	70	31.8		60,000			.7	38.5	44.0	1.20	62.0	78	80	Test stopped before complete fracture.
Average		31.8		60,000			.7	38.8	44.0					
Initially as annealed	110	25.6	3,200 psi/hr.	1.08	500 to 900	18.57 to 19.0				943	19.0	15.0	30.5	Test stopped in second stage.
Extended 9.5% at 250° F. with ultimate of 16,000 psi. Temperature changed to 110° F. at 4,062 hr.	110	25.6	Load added in increments of 1,600 or 3,200 psi. Loading time at 110° F., 1,076 hr.	1.88	500 to 900	23.65 to 24.4				1,680	25.6	20.4	32.2	Do.
Initially as annealed	110	28.8	3,200 psi/hr.	165	24.5 to 105	28.8 to 42.2	105	42.2	40.0	123	62.5	90	278.6	Tested to complete fracture.
Extended 9.8% at 250° F. with ultimate of 16,000 psi. Temperature changed to 110° F. at 4,062 hr.	110	28.8	Load added in increments of 1,600 or 3,200 psi. Loading time at 110° F., 2,756 hr.	2,100	1.2 to 3.03	37.7 to 41.9	3.03	41.9	40.7	5	68.5	86.2	208.6	Do.
Initially as annealed	250	16.0	3,200 psi/hr.	0.44	1103 to 2472	8.34 to 8.94				2,472	8.94	8.19	17.4	Test stopped in second stage.
Do.	250	16.0	Applied instantaneously.	0.43	1108 to 2472	8.43 to 9.01				2,472	9.01	8.34	17.5	Do.
Do.	250	19.2	3,200 psi/hr.	1.43	23 to 123	10.9 to 12.6								Test still in progress.
Do.	250	19.2	3,200 psi/wk.	1.77	1.6	15.1 to 16.5								Test stopped in second stage.
Extended 8.94% at 250° F. with ultimate of 16,000 psi for 2,472 hr.	250	19.2	3,200 psi applied instantaneously.	1.67	759 to 1679	15.05 to 16.54				2,541	18.0	15.3	22.7	Do.
Extended 9% in tensile test at 80° F.	250	19.2	3,200 psi/hr.	1.15	700 to 2200	10.9 to 12.6				2,700	18.0	11.5	21.7	Do.
Initially as annealed	250	22.4	3,200 psi/hr.	10.1	312 to 1248	25.5 to 35.7	1,248	35.7	30.0	1,824	48.9	34.3	34.1	Test stopped in 3d stage before complete fracture.
Extended 18% at 250° F. in 3,381 hr. with ultimate of 19,200 psi.	250	22.4	3,200 psi added instantaneously.	37.8	170 to 369	32.1 to 39.6	369	39.6	31.4	483	47.3	40.5	37.6	Do.
Initially as annealed	250	24.0	3,200 psi/hr.	130	31 to 134	27.9 to 41.2	134	41.2	33.9	168	59.4	78.7	112.4	Tested to complete fracture.
Do.	300	19.2	3,200 psi/hr.	8.3	200 to 990	18.9 to 25.4	990	25.4	24.1	1,522	36.5	33	28.8	Do.
Extended 16.5% at 260° F. in 4,050 hr. with ultimate of 16,000 and 19,200 psi.	300	19.2	Temperature change only, with load on specimen.	8.3	330 to 835	21.2 to 25.4	835	25.4	24.1	1,332	36.5	33	28.8	Do.
Initially as annealed	300	20.9	3,200 psi/hr.	36.4	80 to 335	22.1 to 31.4	335	31.4	27.5	439	46	46.7	39	Do.

III. Results and Discussion

1. Influence of Temperature, Stress, and Rate of Loading on Plastic Extension in First Stage of Creep

The experimental results are summarized in table 1 and figures 1 to 27. The influence of temperature on the stress-strain relationship of the initially annealed copper is shown by a comparison of the relative positions of the curves in figure 1. Except for the specimen extended at 80° F (room temperature) at a rate of 6×10^4 percent/1,000 hr, each specimen was loaded in increments of 3,200 psi applied hourly (hereafter designated as "standard" rate of loading), and the values plotted for extension are those obtained after the application of the loads for a period of 1 hr. Obviously, the resistance to flow decreased as the test temperature was increased. The relatively high resistance to flow of the specimen at 80° F was due partially to the higher strain rate used; an increase in strain rate and decrease in test temperature both tend to increase the rate of work hardening.

Stresses of 3,200 and 6,400 psi produced only small amounts of plastic extension in 1 hr in specimens at 110°, 250°, or 300° F. With the application of higher stresses at each of these temperatures, however, the specimens continued to extend during the 1 hr they were subjected to the constant stress (creep usually occurred at a decreasing rate), as is illustrated by the typical curves given in figure 2 for a specimen tested at 300° F.

The stress-strain curve, for a specimen initially extended 9 percent in tension at room temperature before heating at 250° F for 48 hr and then loaded at the standard rate to an ultimate of 19,200 psi, is given in figure 3. The resistance to plastic deformation at 250° F was materially increased by the cold-working at room temperature. Although the increase in plastic extension at 250° F was less than 0.3 percent after the application of the stress of 19,200 psi for 1 hr, the shape of the curve shows that relatively rapid increases in extension occurred with the application both of the initial and final stresses. The rapid increase in deformation with the application of only 3,200 psi indicates that the internal stress induced by cold-working was considerably relieved during the period of heating at 250° F before applying this stress; the rapid increase in extension with the application of a stress of 19,200 psi may be attributed to a change in grain orientation.

The effect of variations in the rate of loading on the plastic extension at 250° F is shown by the results summarized in figure 4. The experimental points as plotted in this figure are based on the extension produced after the different loads were applied for a period of 1 hr and also at the end of the period of creep when the specimens were allowed to remain under constant loads for periods in excess of 1 hr. At a stress of 16,000 psi, the plastic extension increased somewhat with change in rate of loading

from instantaneous⁴ to increments of 3,200 psi/hr (standard), but the elongation obtained with the standard rate was the same as that of a specimen loaded at a considerably slower rate in increments of 3,200 psi/week. However, the paths of the stress-strain curves of the specimens loaded at the standard (3,200 psi/hr) and slow rates (3,200 psi/week) were not alike. In the early stages of loading, the curve for the specimen loaded relatively slowly was at a higher level (value for extension after load was applied for 1 hr) than that of the curve of the specimens loaded at the standard rate; the stress-strain curves as reproduced for these two specimens either coincide or cross at several points due to the change in plastic extension with increase in time from 1 hr to 1 week at a constant load. At a stress of 19,200 psi, the plastic extension (after 1 hr) of the specimen loaded at the relatively slow rate was greater than that of the specimens loaded at the standard rate, and it was less than that of a specimen loaded at the standard rate to 16,000 psi, allowed to creep at this load for an appreciable time (2,472 hrs) before increasing the stress to 19,200 psi.

The stress-strain curve for a specimen at 110° F, which was loaded at the standard rate, and the curve for another specimen at 250° F on which a stress of 16,000 psi was applied instantaneously are given in figure 5. The stress of 16,000 psi remained on the specimen at 250° F for 4,062 hr (extension of 9.5 percent) before reducing the test temperature to 110° F (load not changed); the test was then continued for 236 hr at 110° F (less than 0.1-percent increase in extension) before increasing the stress to 28,800 psi in increments of either 1,600 or 3,200 psi and allowing to creep at each load for the time as given on the curve. The latter curve falls appreciably below the former curve, especially in the region corresponding to the higher range in stress. Thus the rate of loading to the ultimate and the thermal history had a marked effect on the amount of plastic extension, and this in turn affected the creep rates in the first, second, and third stages, the duration of these stages, and ductility at fracture (table 1).

The results presented in a previous investigation [8] also showed that the creep behavior of initially cold-drawn ingot iron was affected by the rate of loading to the ultimate. The creep rate in the second stage and elongation at fracture both decreased with a decrease in rate of loading in the first stage.

2. Influence of Prior Thermal-Mechanical History on Creep Behavior

A summary of the extension-time curves for the various conditions investigated is given in figure 6, and the influence of prior strain history on creep behavior is shown by a comparison of these curves and those reproduced in figures 7, 8, 9, and 10.

At an ultimate stress of 19,200 psi (fig. 7), the

⁴ The term "instantaneous" is used to designate the rate of loading in which the load was applied gradually over a period of about 30 sec.

general trend was for the creep rate at 250° F to decrease as the rate of attaining the initial extension of about 9 percent was increased. That is, for the same time or strain interval (table 1), the slowest average creep rate during the second stage occurred in the specimen initially extended about 9 percent at room temperature, intermediate in the specimen loaded at the standard rate and extended at 250° F, and next fastest in the specimen allowed to creep 8.9 percent at 250° F (stress of 16,000 psi) before applying a stress of 19,200 psi. The fastest creep rate occurred in the specimen loaded 3,200 psi/week. At 300° F, the average creep rates in the second stage and the extensions both at the beginning of the third stage and at complete fracture were alike for specimens either loaded slowly (allowed to creep at 250° F before increasing the test temperature) or at the standard rate, but the total time required to reach the third stage and fracture was greater for the specimen loaded at the standard (faster) rate.

At an ultimate stress of 22,400 psi (fig. 8), the average creep rate in the second stage at 250° F of the specimen loaded at the standard rate was only about one-quarter of that of another specimen allowed to extend approximately 18 percent at 250° F before applying the ultimate load; the difference in plastic extension at the start of the third stage in the two specimens is partly due to the difference in strain rates in the second stage.

At an ultimate stress of 25,600 psi (fig. 9), the average creep rate in the second stage at 110° F of the specimen loaded at the standard rate was considerably slower than that of the specimen loaded relatively slowly (extended about 9.5 percent in 4,062 hr at 250° F with load of 16,000 psi before decreasing temperature to 110° F and then increasing the load to 25,600 psi in 1,076 hr).

At an ultimate stress of 28,800 psi (fig. 10) the average creep rate in the second stage at 110° F of the specimen loaded at the standard rate (relatively fast) was considerably less than that of another specimen allowed to creep at 250° F and at 110° F with lower stresses before applying the ultimate.

The extension-time curve for a specimen tested at 250° F with an ultimate stress of 22,400 psi into the third stage of creep is reproduced in figure 11. The curve as plotted is typical of the idealized creep in tension (constant load and temperature) in that it consists of an initial extension (about 15 percent) and stages of primary, secondary, and tertiary creep, respectively; the test was discontinued before complete fracture. However, the strain rate during the so-called second stage of approximately constant rate was not constant but varied in a cyclic manner over an appreciable range as is illustrated by the course of the creep rate-time curve given in the upper part of the figure. Even in the primary (creep at a decelerating rate) and tertiary stages (creep at accelerating rate leading to fracture) the change in strain rate with time did not always occur uniformly (continuous decrease or increase, respectively) but often varied in cycles or showed discontinuities in each of these two stages.

Although some irregularities were observed in the creep rate-time relation in each specimen of high-purity copper as tested in tension in creep, the test conditions and prior mechanical history affected the amplitude and frequency of the cycles or discontinuities. For example, the cycles are quite prominent in both the first and second stages for the test conditions as given in figure 9. Cycling is not evident in the first stage in the creep rate-time curve for the specimen tested at an average creep rate of 165 percent per 1,000 hr (fig. 10), or in the third stage of another specimen tested at a creep rate of 2,100 percent per 1,000 hr. The two specimens differed in strain history, which affected the creep rates. It should be pointed out that some cycling or irregularity did occur for each of these conditions, however, the cycling trend is not manifested in the curves until the time coordinate is expanded considerably over that used in figure 10. The phenomenon as observed in the first, second, and third stages is not a direct result of the increase in true stress with increase in plastic deformation during the course of the test as is illustrated for the first and second stages in figure 9.

The effects of test temperature and stress on the cycling of strain rate in the first stage of creep of initially annealed specimens are shown by a comparison of the curves in figure 12. The trend was for the cycling in this stage to decrease in amplitude with increase in both stress and temperature.

As is illustrated in figure 13, the observed trend was for the amplitude of the creep rate-plastic extension cycles in the second stage to decrease with an increase in both the strain rate (constant temperature) and the temperature (constant strain rate). A significant feature is that at a constant temperature, the beginning of this prominent cycling effect was shifted to lower strain values as the ultimate stress was decreased. Furthermore, the amount of plastic extension at the beginning of the second stage of creep decreased with a decrease in ultimate stress. Irregularities are also shown in the creep rate during the first and third stages. However, these irregularities were less prominent in the third than in the first stage and considerably less prominent in both than in the second stage of creep.

The described discontinuities and cycling conditions in the creep rate-time curves are believed to be due to changes in the degrees of slip and the accompanying work hardening and recovery.

Cycling in extension-time curves was also observed and reported in a previous study of the creep characteristics of cold-drawn ingot iron [8].

Any adequate physical theory of the mechanism of the deformation of high-purity copper by creep in tension must account for this variation in strain rate with time or plastic extension.

3. Influence of Prior Strain History on Recovery Characteristics

Carreker, Leschen, and Lubahn [9] investigated the effect of changing stress on strain rate at room temperature of annealed specimens of oxygen-free

high-conductivity copper and high-purity lead wires. A discontinuous change in the strain rate followed by a gradual approach to a steady state value was produced in polycrystalline aggregates of each material when the applied stress was suddenly changed from one to another constant value.

Part of an extension-time curve for a specimen tested at 250° F with an ultimate stress of 16,000 psi is given in figure 14. After the specimen was allowed to extend to about 9.0 percent, the load was removed in increments of 3,200 psi/hr, and when completely unloaded (temperature not changed), it was allowed to rest for 33 hr before starting reloading at the standard rate to an ultimate of 16,000 psi. The specimen was allowed to creep under this stress for an additional period of about 600 hr when the stress was momentarily increased (position *D* on curve); thereafter the specimen continued to creep under the original load. Although the specimen contracted plastically about 0.07 percent during the cycle of unloading and reloading, and extended plastically about 0.06 percent as a result of the momentary increase in stress, the average creep rate in the second stage was not significantly affected by these changes. However, as illustrated by the course of the creep rate-time curve, the amplitude of the cycles increased with these two changes in the testing procedure.

The change in total extension (elastic and plastic) with time as the above specimen was unloaded in steps of 3,200 psi at an interval of 1 hr is shown in figure 15. Although the frequency of the measurements of extension was necessarily decreased in the late stage of each period of 1 hr, the curves as constructed to represent the experimental values show definite trends that are believed to be characteristic. Cycling is evident in each curve except for the condition of zero stress. These cycles are more prominent in the early than in the latter part of the periods after the application of stresses of 12,800 psi, 9,600 psi, or 3,200 psi, and their magnitude appears to decrease with a decrease in stress. Although the specimen contracted after the removal of the loads to attain the stresses of 12,800, 9,600, and 6,400 psi, a noteworthy feature is that the extension increased (not decreased) immediately after the time required to make the initial readings. However, no change in extension was detected immediately after making the initial reading on reducing the stress to 3,200 psi, and at zero load the specimen contracted rapidly for about one-quarter hour, and thereafter, even for a period of 33 hr, its extension was practically unchanged.

The change in total extension of the above specimen after 1 hr under each constant load during unloading and reloading is shown in figure 16. Similar curves are also reproduced for unloading two other specimens at 250° F at the same rate (3,200 psi/hr) from an ultimate of 19,200 psi. As is shown by the difference in slope of the curves, the prior strain history of the specimens affected the degree of recovery at 250° F during unloading; the decrease in total extension for the three specimens at zero

load ranged from about 0.2 percent for the specimen unloaded from 16,000 psi to about 0.3 percent for the two specimens unloaded from 19,200 psi.

4. Influence of Temperature and Stress on the Average Creep Rate in the Second Stage

The relation between nominal stress and average creep rate in the second stage of specimens tested at different temperatures is shown in figure 17. At 250° F, the experimental values do not fall on a straight line in either a semilog or log-log plot. The course of the stress-strain rate curve was not definitely established at 110° or 300° F as only two creep tests were made at each of these temperatures. However, these results show that the resistance to creep of the initially annealed copper increased with a decrease in test temperature.

5. Variation of Ductility with Temperature and Creep Rate

In the creep tests in which the specimens were loaded at the standard rate the initial extension, intercept, extension at the start of the third stage, extension at fracture, and reduction of area at fracture (fig. 18) each increased with an increase in strain rate (constant temperature) and tended to decrease with an increase in temperature (constant strain rate). It should be pointed out, however, the extension at fracture of the specimen tested in creep at 110° and 250° F was greater than that of the specimens fractured at room temperature in the ordinary tension test (table 1). The true stress at complete fracture of the specimen tested at 110° F (strain rate of 165 percent per 1,000 hr) was also considerably greater than that of the specimens fractured at room temperature. This increase is believed to be due in part to the higher strain rate just prior to complete fracture of the specimen tested in creep.

6. Influence of Prior Thermal Mechanical History on Room Temperature Tensile and Hardness Values

The effect of plastic extension in creep at 110° and 250° F on the flow characteristics at 80° F (room temperature) is shown in figure 19. The true stress-strain curves at 80° F (based on total deformation) for the specimens initially as annealed or extended into the second stage of creep at rates of about 1.1 percent per 1,000 hr are nearly alike over the range in true stress of 40,000 to 70,000 psi. That is, the combined effect of creep, work-hardening, and recovery at 110° or 250° F is not manifested in the shape of the flow curves in this range of stress. The true stress-strain curve at 80° F of the specimen extends into the third stage of creep at 250° F (49% extension at a rate of 10%/1,000 hr) falls appreciably below the corresponding curve of the annealed material. The lowering of the flow curve for this specimen previously extended in creep can be attributed to its relatively high degree of recovery and

possibly to the presence of cracks of submicroscopic dimensions at the completion of the creep test (fig. 23, D and E).

In all cases, the values at maximum load for plastic extension, reduction of area, and true stress were less in the annealed specimen than the corresponding values of the specimens previously extended in creep. However, the values for reduction of area and true stress at both the beginning of and at complete fracture were less for each of the specimens previously extended in creep at 250° F than those of the annealed specimens or the specimens extended in creep at 110° F.

The change in hardness at room temperature with plastic extension (reduction of area) of specimens tested to complete fracture in creep at different temperatures and rates, and in tension at room temperature, is given in figure 20. The hardness of the initially annealed specimens ($R_p=34$) increased markedly with increase in plastic deformation to the third stage of creep (20 to 30 percent reduction of area, table 1); thereafter the induced hardness varied with the amount of deformation, temperature of deformation, and strain rate. Of the two specimens tested at 300° F, the induced hardness was somewhat greater and the peak in the hardness-reduction of area curve occurred at a greater amount of extension in the specimen tested at the higher strain rate in the second stage. In both specimens, the value for hardness in the vicinity of the fracture was less than that at some lower value of extension. The curves for the specimen tested in ordinary tension at 70°, and in creep at 110° and 250° F, were quite similar in that none showed a definite break or peak (that is, the maximum hardness is in vicinity of fracture), and the maximum hardness value attained in each was greater than that of the specimens tested in creep at 300° F. In the plastic range beyond the beginning of the third stage, however, the curve for the specimen tested at 250° F is below the curves of the specimens at 80° and 110° F.

7. Changes in Microstructure and Fracture Characteristics as Affected by Temperature and Strain Rate

For the specimens tested to complete fracture in creep, the propensity to necking (fig. 21) and to transcrystalline fracture (fig. 22) increased with increase in strain rate and decrease in temperature. At sufficiently high strain rates and low temperatures, considerable necking occurred (fig. 21, A, B, and C) and the fractures were essentially transcrystalline (fig. 22, B, C, and D), but with relatively slow strain rates and high temperatures no appreciable necking occurred (fig. 21, D, E, and F) and the fractures were predominantly intercrystalline (fig. 22, E and F). In the specimens that fractured in a transcrystalline manner (fig. 22, B and C), cracking was confined principally to the region of complete fracture, whereas in the specimens that fractured in an intercrystalline manner (fig. 22, E and F) numerous cracks (general disintegration) were observed in regions remote from complete fracture; some cracks of microscopic dimen-

sions were observed about 0.05 in. from the position of complete fracture of a specimen in which the fracture appeared to be partly intercrystalline but predominantly transcrystalline (fig. 22, D).

The tendency for a specimen to disintegrate as plastic deformation by creep proceeds to intercrystalline rupture is illustrated by a comparison of typical photomicrographs of figures 22, F, and 23, A and B. Appreciable cracking is evident even at a deformation corresponding to the beginning of the third stage of creep (fig. 23, B) in a specimen tested at 300° F to complete rupture. Similar conditions were observed in another specimen fractured in creep at the same temperature (300° F) and strain rate (8.3%/1,000 hr) but with an entirely different strain history. Furthermore, cracking at deformations corresponding to the beginning of the third stage of creep was detected in two other specimens tested at a lower temperature (250° F) and different strain rates (fig. 23, C and D). The creep tests of the latter two specimens were terminated during the third stage before complete fracture, but one specimen was subsequently fractured at 80° F.

Only a few cracks of microscopic size were observed at a deformation corresponding to the beginning of the third stage in the specimen extended in creep at 250° F and finally fractured at 80° F (fig. 23, D). Although these cracks were located principally in the interior of the specimen in the vicinity of its axis, a few cracks were also located at the surface (fig. 23, E). The surface cracks (not detected at a magnification of about 25 diameters) were invisible at the end of the creep test. As previously shown (fig. 19), the true stress-strain curve at 80° F of this specimen was materially lowered by extending in creep, and this decrease in resistance to flow might be partly due to the presence of submicroscopic cracks at the termination of the creep test.

It is evident, therefore, that under certain conditions the third stage of creep can be accompanied by cracking, but other evidence (fig. 22, C) shows that cracks of microscopic dimensions are not a prerequisite for the initiation of the third stage of creep in high-purity copper.

Baeyeritz, Craig, and Bumps [10] reported the presence of discontinuous cracks in steel fractured by impact, and Jaffee, Reed, and Mann [11] also found discontinuous cracks adjacent to the path of final brittle failure in both fatigue and impact specimens made from steel forgings and castings. Tipper [12] observed microcracks near the fracture of mild steel plates. Jaffee and coauthors [11] were of the opinion that brittle transgranular fracture of polycrystalline metal does not originate at one point and propagate continuously across the material, but rather nucleate at numerous related points, leading to a series of microcracks that link up subsequently.

In some cases, cracking leading eventually to complete fracture was initiated at the axis of specimens tested in tension, whereas in other specimens cracking was initiated at the surface. As is illustrated in figure 24 and 25, the position (interior or exterior of the specimen) where cracking was initiated and the

course of the propagation of these cracks depended upon the test conditions, such as strain rate and temperature. In a specimen extended in ordinary tension at 80° F until the true stress-strain curve indicated the beginning of fracture (fig. 24, *A*), cracking started at or near the axis of the necked section (fig. 24, *B*), and had the specimen been carried to complete rupture these discontinuous cracks (fig. 25, *A*) would have linked up as they propagated transcrystallinely outward to the surface (fig. 22, *B*); no cracking was visible at the surface of the neck section of this specimen (fig. 25, *B*). In such failures, appreciable necking occurs and the "so-called breaking or fracture stress" is usually considerably higher than the true-fracture stress (fig. 19) due to the "rim effect."

Microcracking was confined to the immediate vicinity of complete fracture of another specimen, which was extended 9 percent in tension at 80° F prior to testing into the second stage of creep at 250° F (additional extension of 7%) and finally fracturing at 80° F (fig. 23, *F*). As considerable necking with its accompanying rim occurred and the fracture was transcrystalline, it is believed that cracking was initiated near the axis of the specimen and not at its surface. That is, the creep test was carried out under conditions that did not nucleate at the surface a crack that subsequently propagated across the entire specimen. However, in a specimen extended at 250° F at creep rates of about 1.5 and 37.8 percent per 1,000 hr (to extension of 18 and 47%, respectively), cracking was initiated at the surface (figs. 24, *C, D*; 25, *C, D, E*), but evidently cracking subsequently commenced in the interior (fig. 25, *F*); the numerous small cracks observed in the interior after a light etch (not clearly shown in fig. 25, *F*) appear to have originated principally at the grain boundaries. In such failures, only a small amount of necking occurs, and the path of the fracture is predominantly intercrystalline.

Wilms and Wood [13] described a mechanism by which metals deform at normal and elevated temperatures. At normal temperatures, deformation occurs mainly by the mechanism of slip and the break-down of the grains to crystallites of submicroscopic size. As the temperature is raised and the rate of deformation is diminished, this mechanism is increasingly replaced by one in which the grains dissociate into comparatively coarse units and permit flow by the relative movement of these units within the parent grain. The units, which are termed "cells", can be observed and measured. They are considered to be responsible for the continuous deformation under stress, which characterizes the phenomenon of creep.

Some changes in structural features accompanying plastic deformation of high-purity copper in ordinary tension and in creep at different temperatures are shown in figures 26 and 27. A lineage structure is evident in the equiaxed grains in the initially annealed specimen (fig. 26, *A*). These grains were elongated in the direction of the applied stress during the process of deforming in tension, and the degree

of distortion in this direction depended upon the amount of plastic extension, strain rate, and temperature. Relatively high strain rates and low temperatures both favored this condition, and the elongation of the grains usually attained a maximum at or in the vicinity of complete fracture. The break-down of the original grains as plastic deformation proceeds is also evident by the presence of a substructure that appears to be numerous crystals of microscopic dimensions within certain of the parent grains. Although the number and size of these subcrystals appear to be affected by the amount of plastic extension and test conditions, they were observed in specimens tested under a wide range of conditions (compare fig. 26, *B*, and fig. 27, *B*). The general trend was for the size of the subcrystals to increase with increase in test temperature and decrease in strain rate.

In a study of the changes in microstructure of single and polycrystalline aluminum plastically deformed at different temperatures and strain rates, Hanson and Wheeler [14] observed slip bands (specimen polished prior to deforming) on the surface of single crystals at all temperatures and strain rates used. With polycrystalline specimens, the slip bands without marked changes at the grain boundaries, were observed when the specimens were strained at relatively high rates and low temperature (ordinary tension at room temperature) but were not visible in the specimens tested in creep at relatively slow rates and high temperature. In the latter specimens that did not exhibit slip bands, marked localized deformation occurred at or near the grain boundaries, and fracture was intercrystalline without necking.

Strain markings were quite prominent in all of the copper specimens carried to complete fracture, regardless of the testing conditions used (figs. 26 and 27). The markings in some of the parent grains have the appearance of twins, even in the vicinity of incipient cracking, as is illustrated in figure 27, *A*, for a specimen extended at the highest temperature used (300° F) with a strain rate of only 36.4 percent per 1,000 hr.

IV. Summary

Creep tests in tension were made at various temperatures and strain rates on initially bright annealed oxygen-free high-conductivity (OFHC) copper. The testing program included a study of the influence of thermal and strain history, rate of loading to the ultimate, sudden change in stress from one to another constant value, and change in test temperature on creep behavior and plastic deformation. Metallographic examinations and hardness measurements were carried out at room temperature on specimens representative of the copper before and after testing in creep. In addition, tensile tests provided data on true-stress-strain relations at room temperature on specimens as annealed or as previously extended at elevated temperatures into the second or third stage of creep.

The prior thermal and strain history and rate of loading to the ultimate affected markedly the amount

of plastic deformation and creep behavior. The general trend was for the degree of plastic deformation and creep rate in the second stage to decrease as the rate of loading was increased.

The strain rate during the second stage of creep was not constant but varied with time in a cyclic manner. The trend was for the amplitude of these cycles to decrease with increase in both stress and temperature.

In some cases, the beginning of the third stage of creep was accompanied by cracks of microscopic dimensions, but the presence of such cracks are not a prerequisite for the initiation of the third stage of creep in high-purity copper.

The positions at which cracks were nucleated and the course of their propagation were affected by the test conditions. Cracking started at or near the axis of the specimen tested in ordinary tension at room temperature. These discontinuous cracks united as they propagated transcrystallinely outward toward the surface, and appreciable necking occurred in the specimen before complete rupture. Cracking started at the surface of a specimen tested into the third stage of creep at 250° F, but at a later stage numerous small cracks were also nucleated in its interior, principally in the parent grain boundaries. Complete rupture occurred in this specimen without appreciable necking and the fracture was predominantly intercrystalline.

The degree of necking, ductility at the beginning of the third stage and at complete rupture, and the propensity to transcrystalline fracture of the specimens tested in creep increased with an increase in strain rate (temperature constant) and with a decrease in temperature (strain rate constant).

Metallographic examination showed the breakdown of the original grains of the copper that occurred with plastic deformation under a wide range of test conditions. Strain markings were also observed in all specimens that were carried to complete rupture. Some of these markings had the appearance of twins.

The authors are indebted to J. H. Darr, C. R. Johnson, and F. A. Wilkinson for assistance in making many of the measurements of creep.

V. References

- [1] D. J. McAdam, Jr., G. W. Geil, and D. H. Woodard, Influence of strain rate and temperature on the mechanical properties of Monel metal and copper, *Proc. Am. Soc. Testing Materials* **46**, 902 (1946).
- [2] E. R. Parker and C. F. Riisness, Effect of grain size and bar diameter on creep rate of copper at 200° C, *Metals Tech.* **11**, TP 1690 (Feb. 1944); *Trans. Am. Inst. Mining Met. Engrs. (Inst. of Metals Div.)* **156**, 117 (1944).
- [3] E. R. Parker, The effect of impurities on some high temperature properties of copper, *Trans. Am. Soc. Metals* **29**, 269 (1941).
- [4] E. A. Davis, Creep and relaxation of oxygen-free copper, *Trans. Am. Soc. Mech. Engrs.* **65**, [A] 101 (1943).
- [5] H. L. Burghoff and A. I. Blank, The creep characteristics of copper and some copper alloys at 300, 400, and 500° F, *Proc. Am. Soc. Testing Materials* **47**, 725 (1947).
- [6] A. D. Schwöpe, K. F. Smith, and L. R. Jackson, The comparative creep properties of several types of commercial coppers, *J. Metals* **1**, (July 1949); *Metals Trans.* **185**, 409 (1950).
- [7] J. A. Bennett and D. J. McAdam, Jr., Creep rates of cold-drawn nickel-copper alloy (Monel metal), *J. Research NBS* **28**, 417 (1942) RP1462.
- [8] W. D. Jenkins and T. G. Digges, Influence of strain rate and temperature on the creep of cold-drawn ingot iron, *J. Research NBS* **43**, 117 (1949) RP2013.
- [9] R. P. Carreker, J. G. Leschen and J. D. Lubahn, Transient plastic deformation, *Trans. AIME (Inst. of Met. Div.)* **180**, 139 (1949); *Metals Tech.* **15** (Sept. 1948) TP2477.
- [10] M. Baeyeritz, W. F. Craig, Jr., and E. S. Bumps, A metallographic description of fracture in impact specimens of a structural steel, *J. Metals* **1** (August 1949); *Metals Trans.* **185**, 481 (1950).
- [11] L. D. Jaffe, E. L. Reed, and H. C. Mann, Discontinuous crack propagation—Further studies, *J. Metals* **1** (Oct. 1949); *Metals Trans.* **185**, 683 (1950).
- [12] C. F. Tipper, Brittle fracture in mild-steel plates II, *Engineering* **165**, 594 (1948).
- [13] G. R. Wilms and W. A. Wood, Mechanism of creep in metals, *J. Inst. Metals* **75**, 693 (1949).
- [14] D. Hanson and M. A. Wheeler, The deformation of metals under prolonged loading. I—The flow and fracture of aluminium, *J. Inst. Metals Proc.* **45**, 229 (1931).

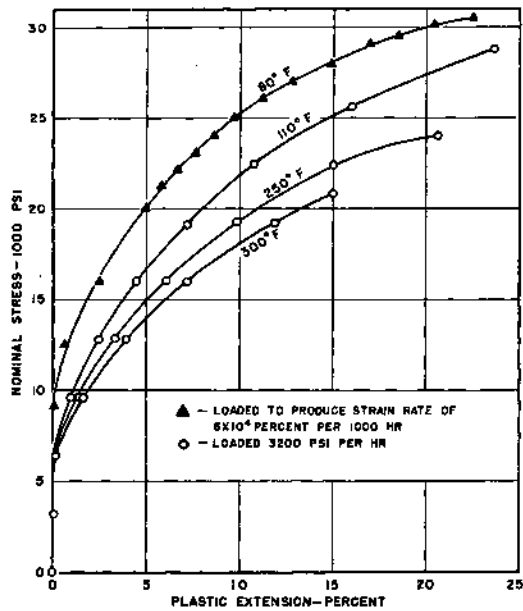


FIGURE 1. Effect of nominal stress on plastic extension at different temperatures.

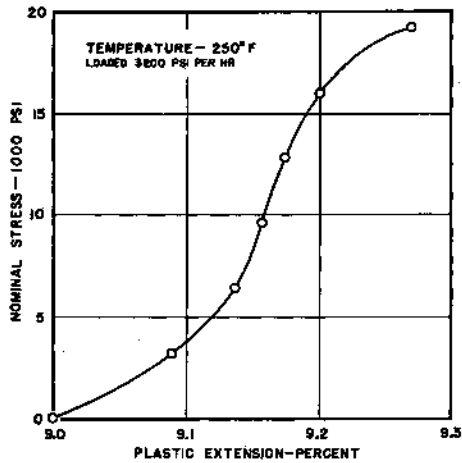


FIGURE 3. Effect of nominal stress on plastic extension at 250° F.

The specimen was initially extended 9 percent in tension at 80° F. The values for extension are those obtained 1 hour after the application of the loads.

FIGURE 5. Effect of rate of loading and prior thermal-mechanical history on plastic extension at 110° F.

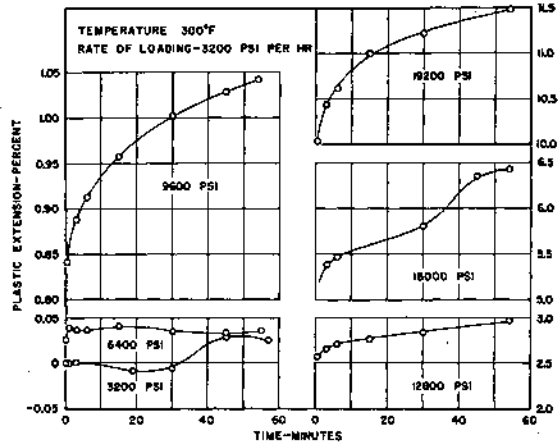


FIGURE 2. Variation in plastic extension with time at 300° F with different nominal stresses.

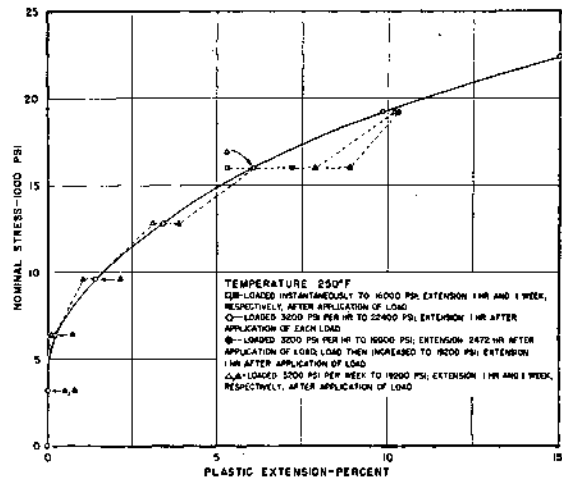
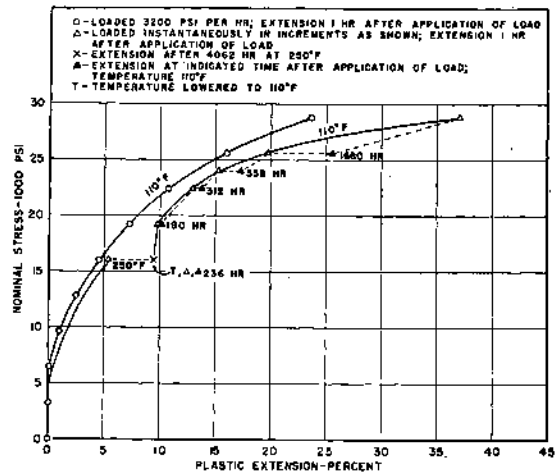


FIGURE 4. Effect of rate of loading on plastic extension at 250° F.



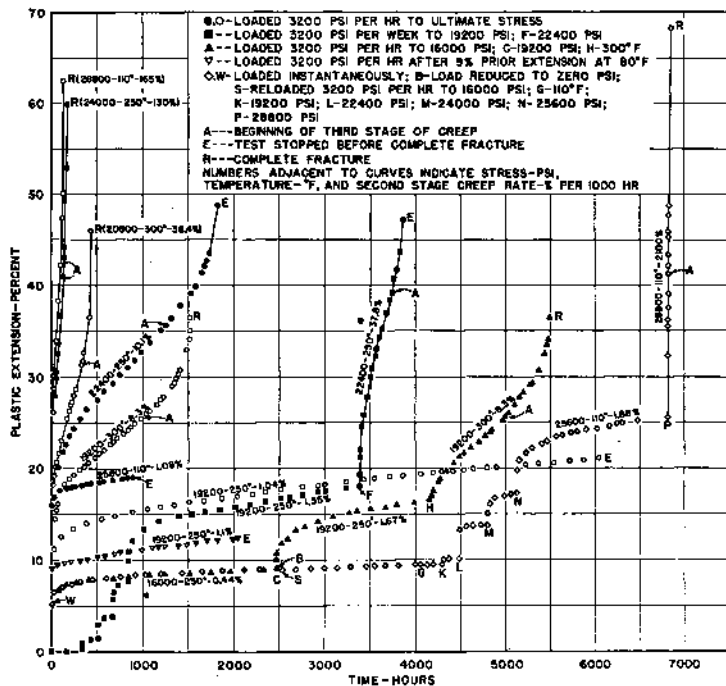


FIGURE 6. Summary of extension-time curves for specimens tested in creep under the various conditions used.

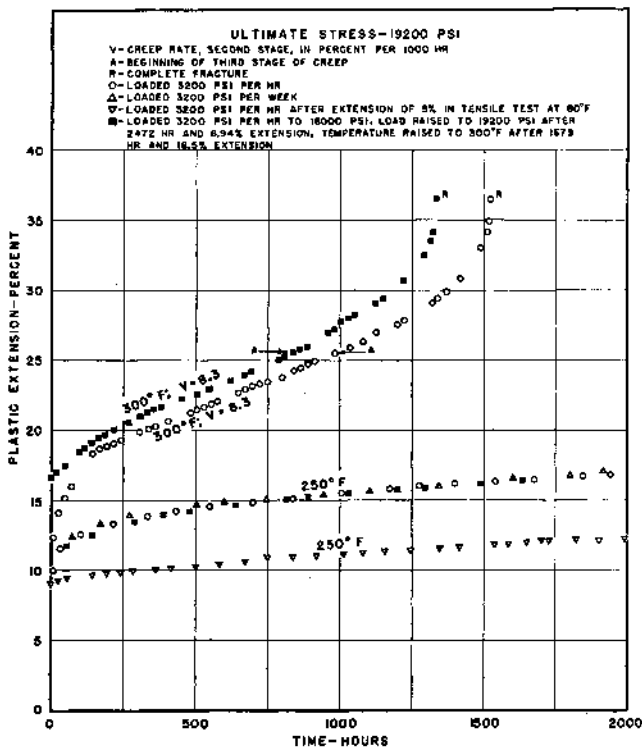


FIGURE 7. Effect of rate of loading on creep at 250° and 300° F.

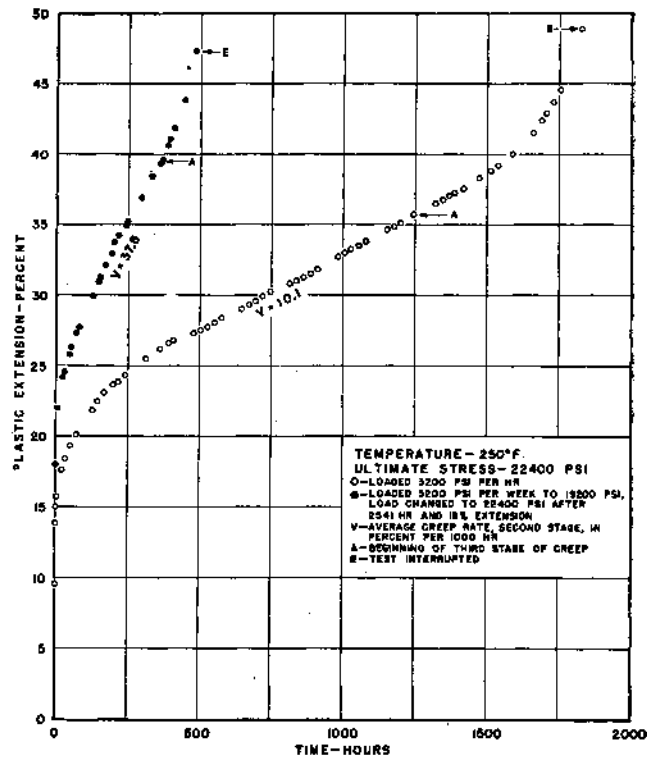


FIGURE 8. Effect of rate of loading on creep at 250° F.

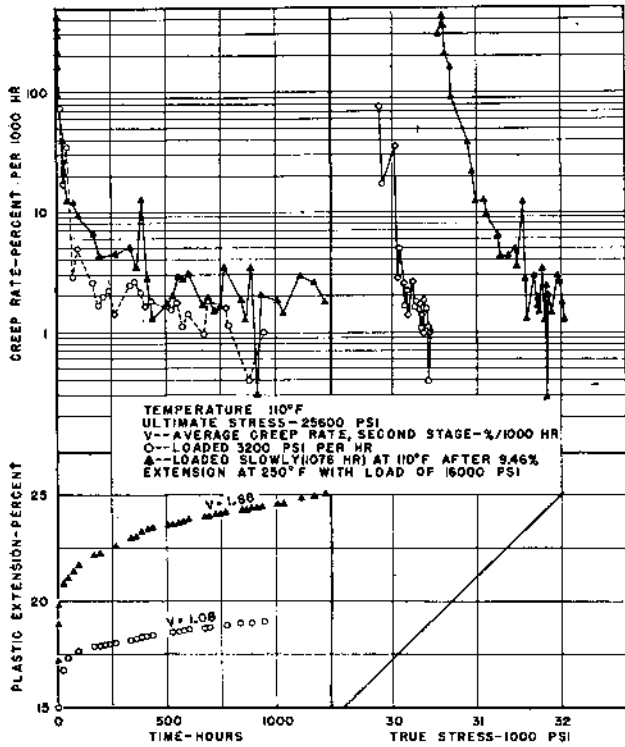


FIGURE 9. Effect of rate of loading on creep at 110° F.

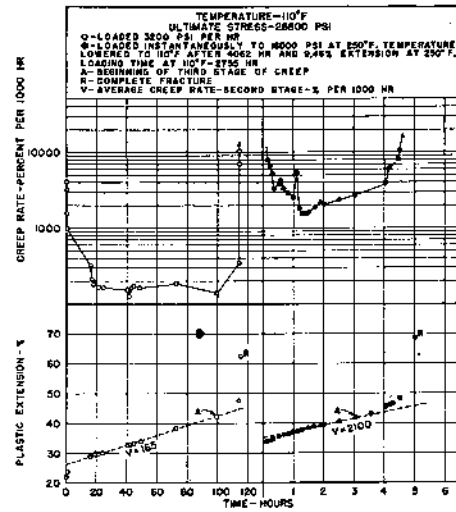


FIGURE 10. Effect of rate of loading on creep at 110° F.

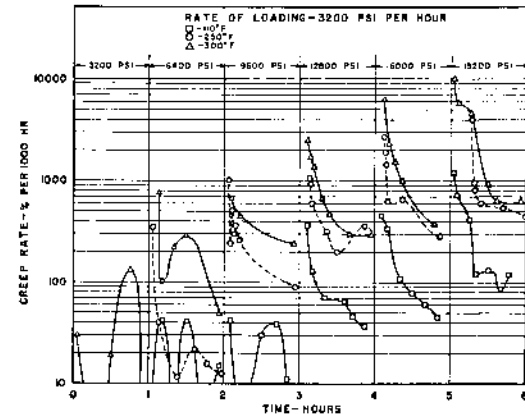
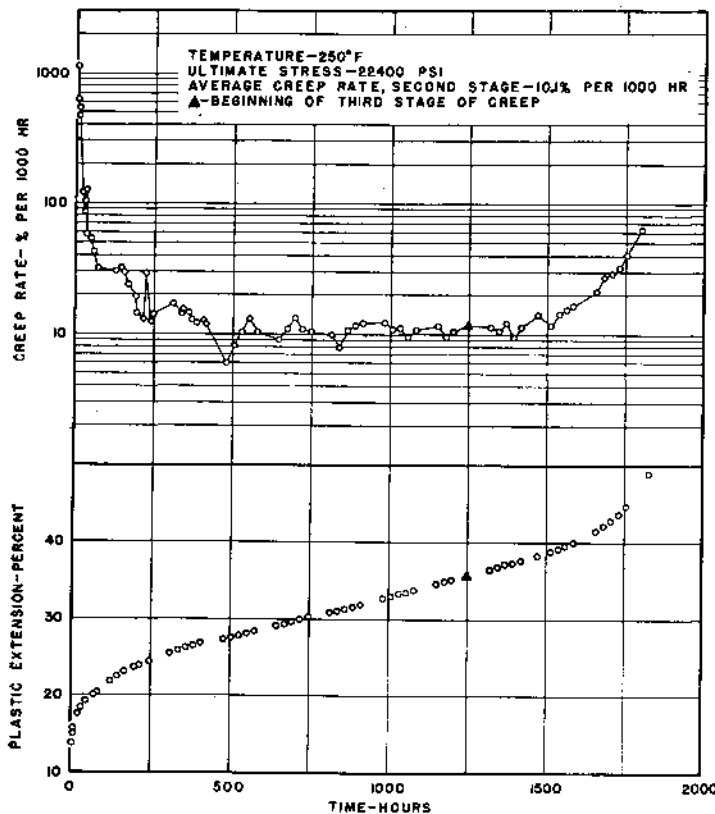


FIGURE 12. Variation in creep rate in the first stage with time at different temperatures and with different nominal stresses.

FIGURE 11. Extension-time and creep rate-time relations for a specimen tested at 250° F with a nominal stress of 22,400 psi.

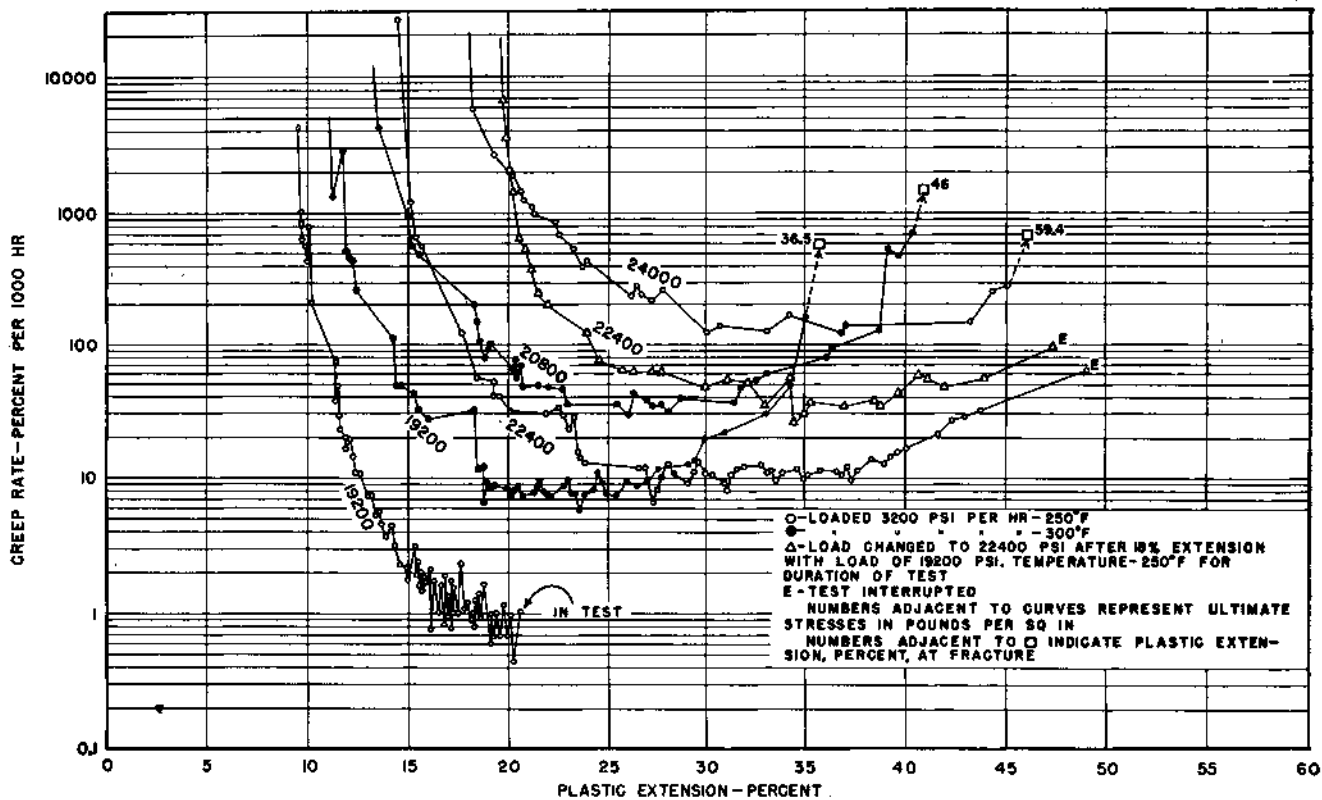


FIGURE 13. Variation in creep rate with plastic extension at 250° and 300° F.

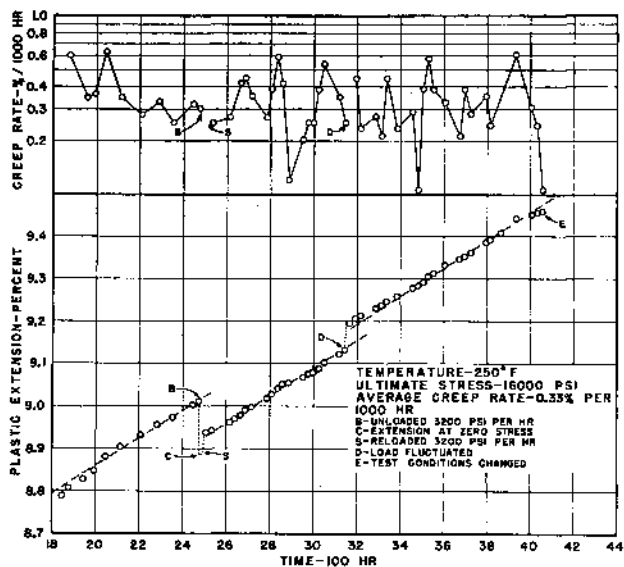


FIGURE 14. Variations in plastic extension and creep rate with time at 250° F.

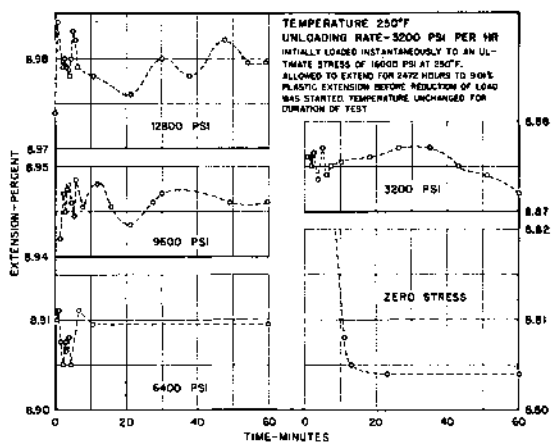


FIGURE 15. Change in extension with time at 250° F of a specimen unloaded from 16,000 psi.

Some creep characteristics of this specimen before and after unloading and reloading are given in figure 14.

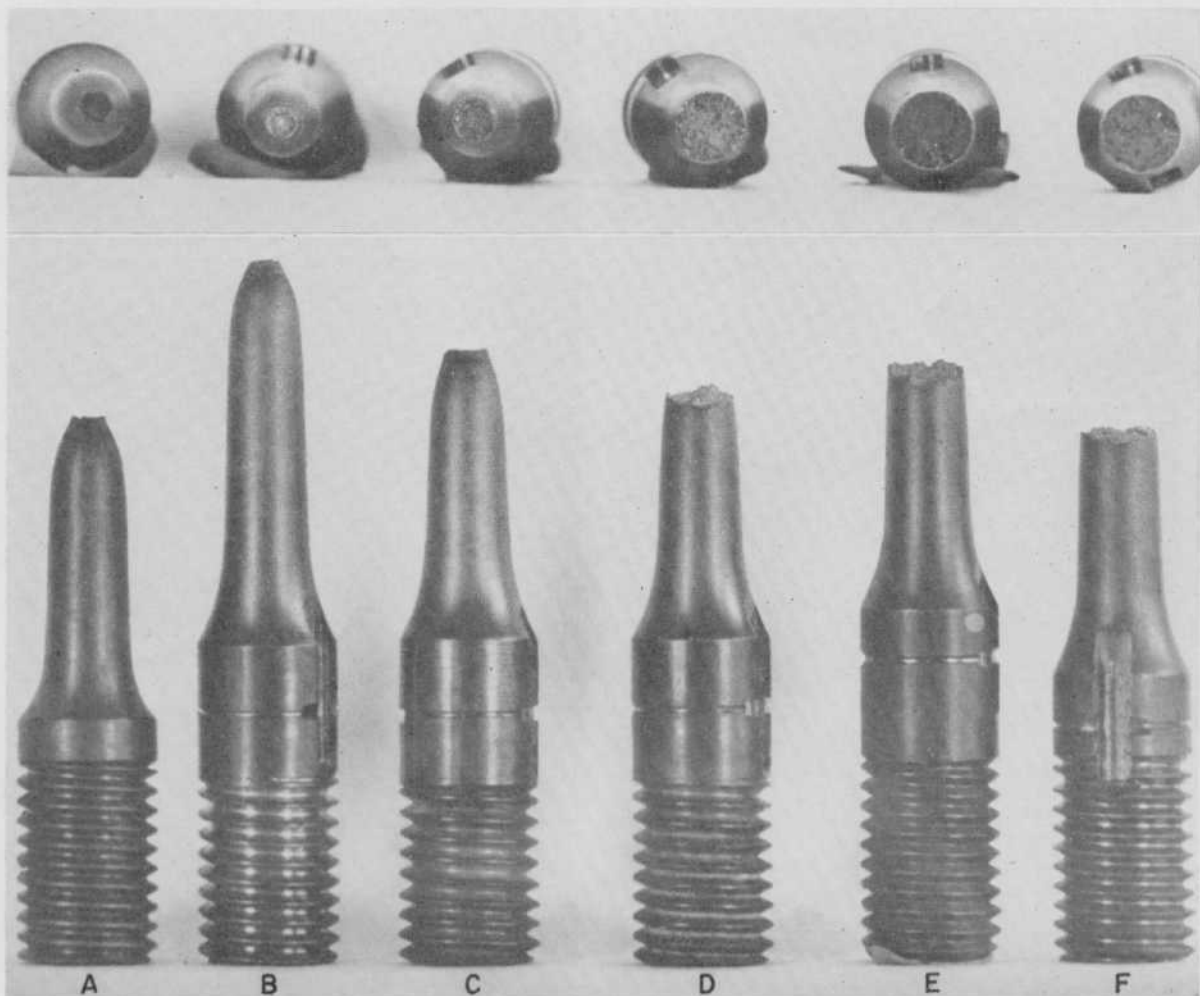


FIGURE 21. Specimens after fracturing at different temperatures and rates; $\times 1$.

	Test					Test			
	Temperature	Strain rate	Elongation in 2 in.	Reduction of area		Temperature	Strain rate	Elongation in 2 in.	Reduction of area
	$^{\circ}F$	%/1,000 hr	%	%		$^{\circ}F$	%/1,000 hr	%	%
A-----	80	60,000	51.0	88	D-----	300	36.4	46.0	47
B-----	110	165	62.5	90	E-----	300	8.3	36.5	29
C-----	250	130	59.4	79	F-----	300	8.3	36.5	29

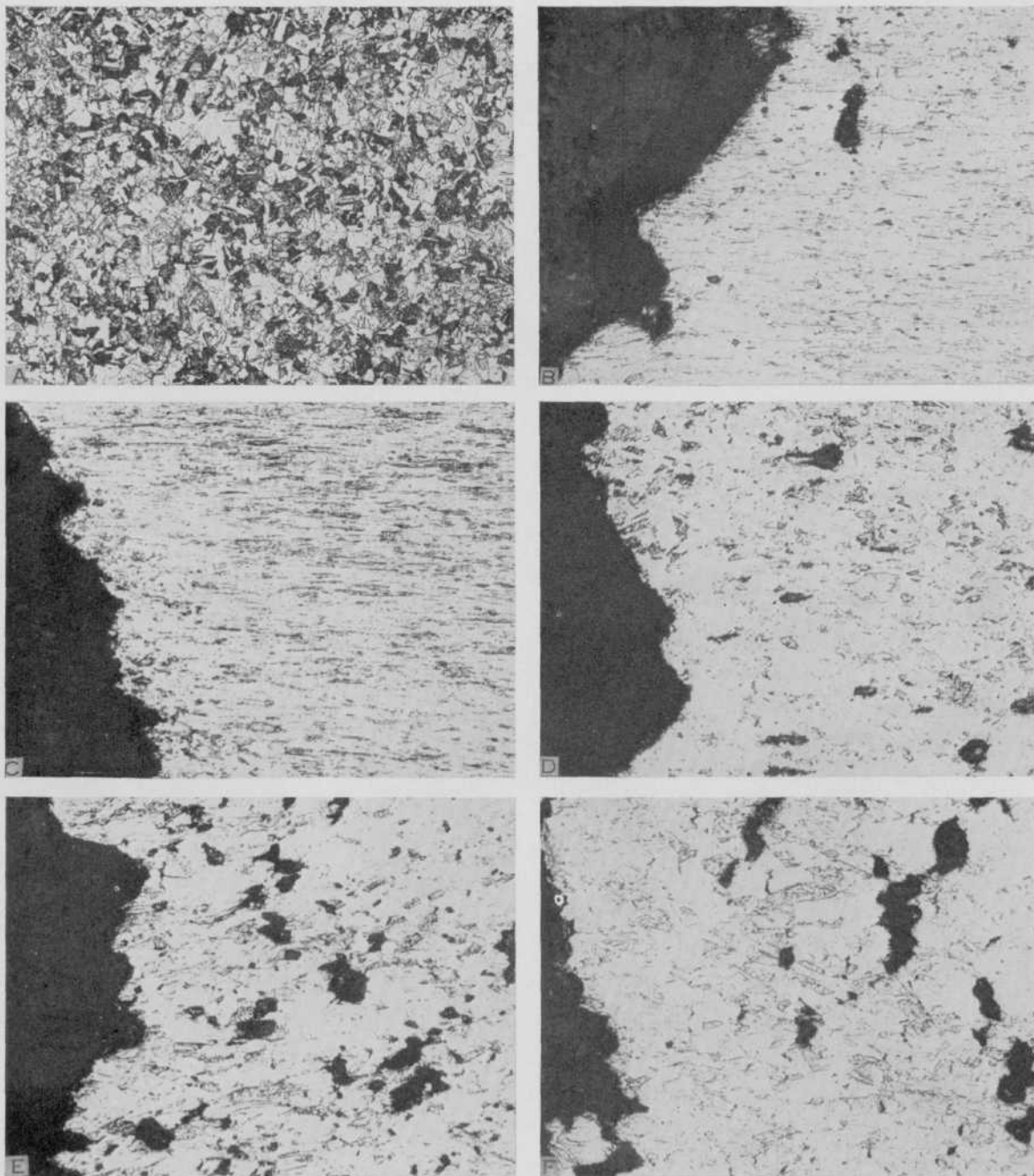


FIGURE 22. Grain size of annealed copper and structures at fracture of specimens tested at different temperatures and rates.

Longitudinal sections etched in equal parts NH_4OH and H_2O_2 (3%).

	Test		Elongation in 2 in.	Reduction of area	Remarks
	Temperature	Strain rate,			
	$^{\circ}\text{F}$	%/1,000 hr	%	%	
A					$\times 75$; as annealed; 0.025-mm diam of average grain.
B	80	60,000	51.0	88	$\times 100$.
C	110	165	62.5	90	$\times 100$.
D	250	130	59.4	79	$\times 100$.
E	300	36.4	46.0	47	$\times 100$.
F	300	8.3	36.5	29	$\times 100$.

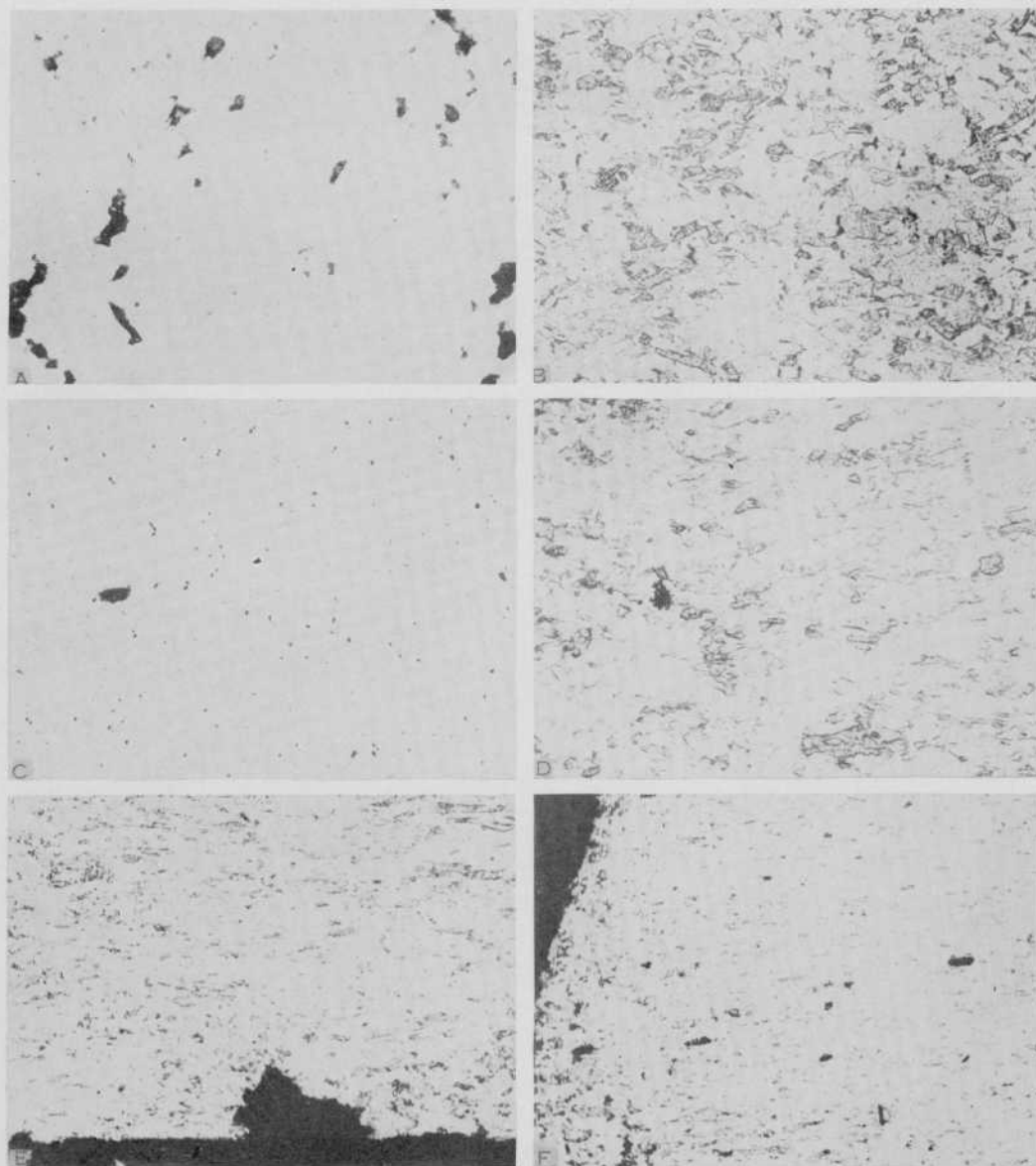


FIGURE 23. *Effect of temperature, rate, and plastic deformation on microcracking.*

Longitudinal sections near axis of specimen, except as indicated, etched in equal parts of NH_4OH and H_2O_2 (3%). Original magnification, $\times 100$ (reduced one-tenth in reproduction).

	Test		Remarks
	Temperature	Strain rate	
A.....	300	8.3	Structure 0.05 in. from complete fracture. Structure at fracture is shown in fig. 22, F.
B.....	300	8.3	Same specimen as above, structure at deformation corresponding to the beginning of third stage.
C.....	250	1.5(a)	(a) 19,200 psi for 2,540 hr; (b) 22,400 psi for 483 hr; stopped in third stage; structure at deformation corresponding to the beginning of third stage.
D.....		37.8(b)	
E.....	250	10.1	Stopped in third stage; fractured at room temperature; structure at deformation corresponding to the beginning of third stage.
F.....	250	10.1	Same specimen as above; structure at surface 0.05 in. from complete fracture.
	250	1.15	Extended 9% at room temperature; 19,200 psi at 250° F for 2,700 hr; stopped in second stage and then fractured at room temperature; structure at complete fracture.

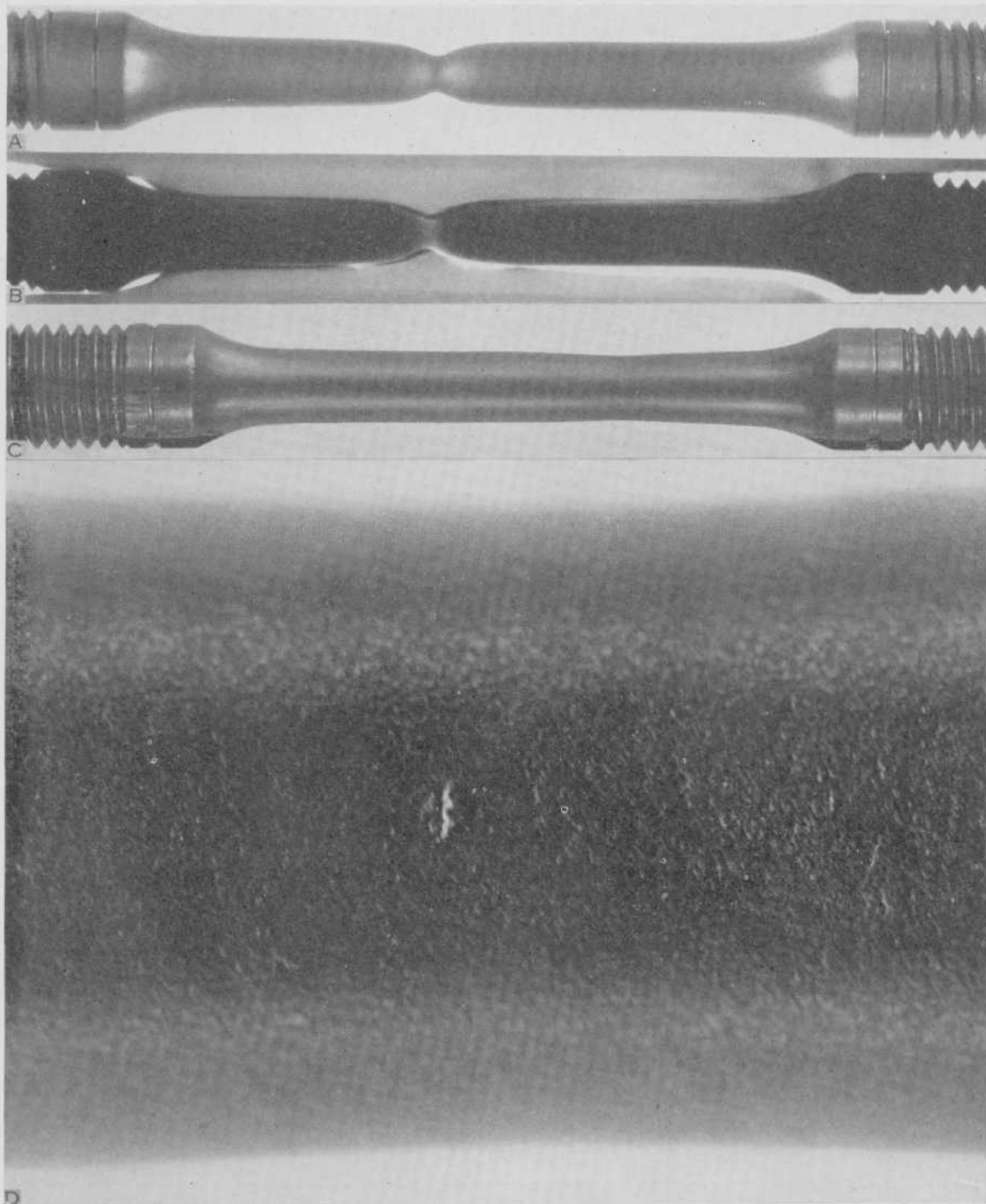


FIGURE 24. Photographs and radiograph of specimens after testing at different temperatures and rates.

	Test		Remarks
	Temperature	Strain rate	
	$^{\circ}F$	%/1,000 hr	
A.....	80	60,000	Photograph, $\times 1$.
B.....	80	60,000	Radiograph of above specimen, indicating the presence of a crack in the necked section.
C.....	250	{ 1.5 (a)	(a) 19,200 psi for 2,540 hr; (b) 22,400 psi for 483 hr; photograph $\times 1$.
		{ 37.8 (b)	
D.....	250	{ 1.5	Photograph, $\times 10$ of above specimen showing the presence of a crack at the surface of the necked section.
		{ 37.8	

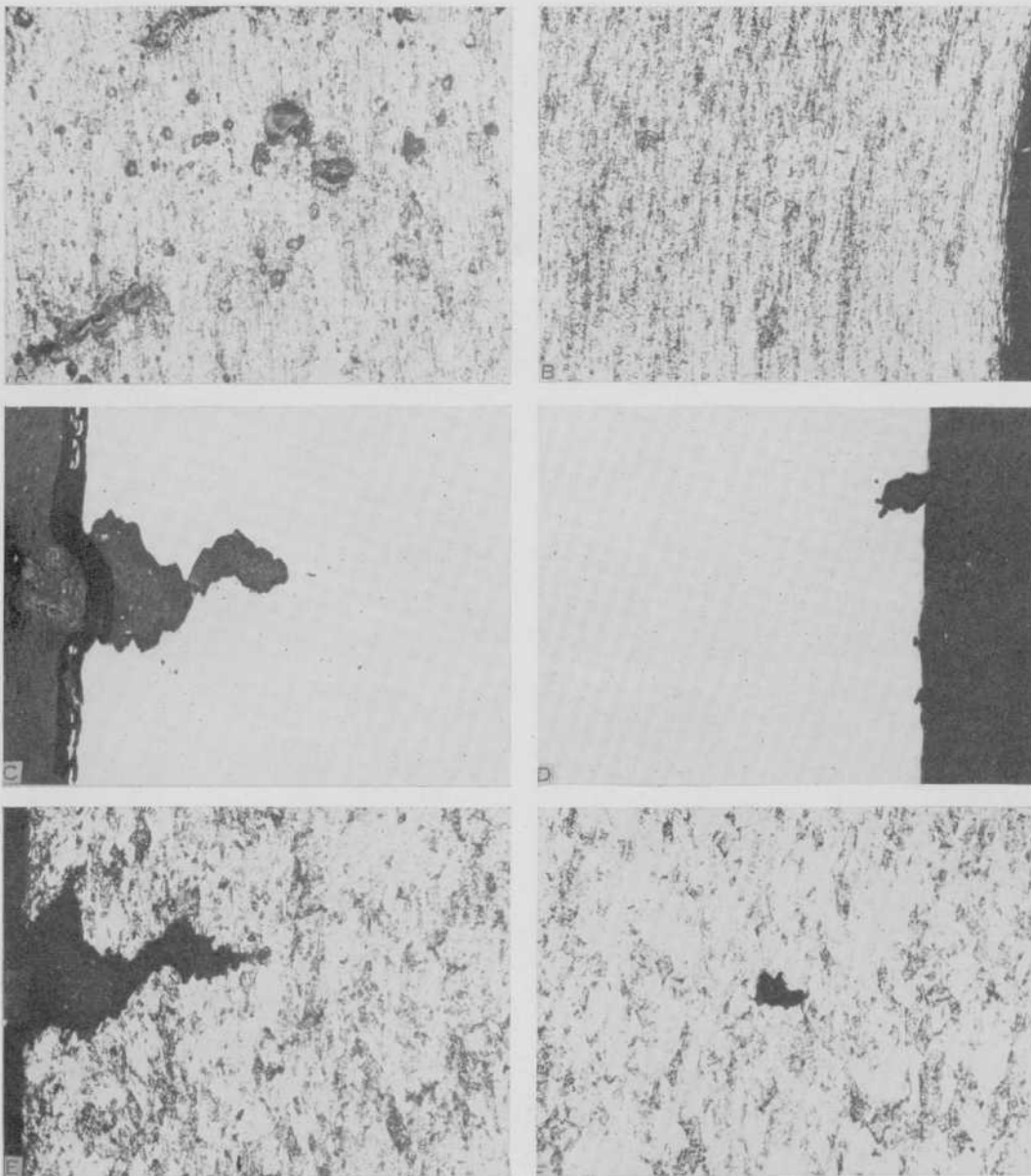


FIGURE 25. Effect of testing conditions on the initiation of microcracks.

Longitudinal sections, *A*, *B*, *E*, and *F* etched in equal parts NH_4OH and H_2O_2 (3%). *C* and *D* unetched. Original magnification, $\times 100$ (reduced one-tenth in reproduction).

	Test		Remarks
	Temperature	Strain rate	
	$^{\circ}\text{F}$	%/1,000 hr	
<i>A</i>	80	60,000	Structure at the axis of necked section of specimen shown in fig. 24, <i>A</i> and <i>B</i> . Structure at the surface of the necked section of above specimen.
<i>B</i>	80	60,000	
<i>C</i>	250	1.5	Structure at the surface of necked section of specimen shown in fig. 24, <i>C</i> and <i>D</i> .
<i>D</i>		37.8	
<i>E</i>	250	1.5	Same as <i>C</i> , except that the surfaces are diametrically opposite.
<i>F</i>		37.8	
	250	1.5	Same section as <i>C</i> , after etching.
		37.8	
	250	1.5	Same section as <i>C</i> , structure at the axis of the specimen.
		37.8	

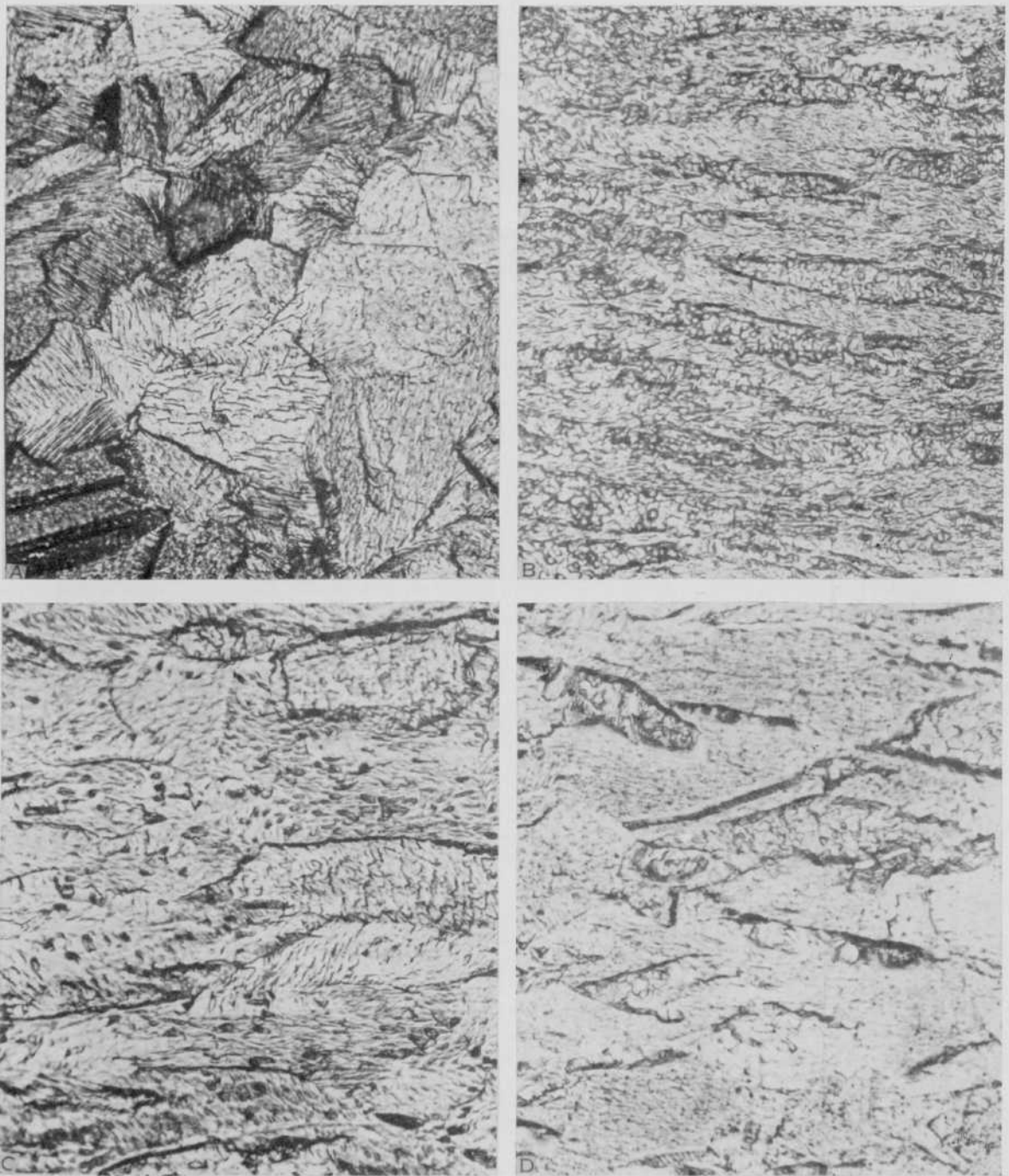


FIGURE 26. *Effect of testing conditions on the structure of copper initially as annealed.*

Longitudinal sections etched in 3.5 parts glacial acetic acid, 4.5 parts nitric acid (conc.), and 2 parts absolute alcohol, $\times 750$.

	Test		Remarks
	Tempera- ture	Strain rate	
	$^{\circ}F$	%/1,000 hr	
A.....			As annealed.
B.....	80	60,000	Structure near axis of specimen 0.10 in. from position of complete fracture.
C.....	110	165	Do.
D.....	250	130	Do.

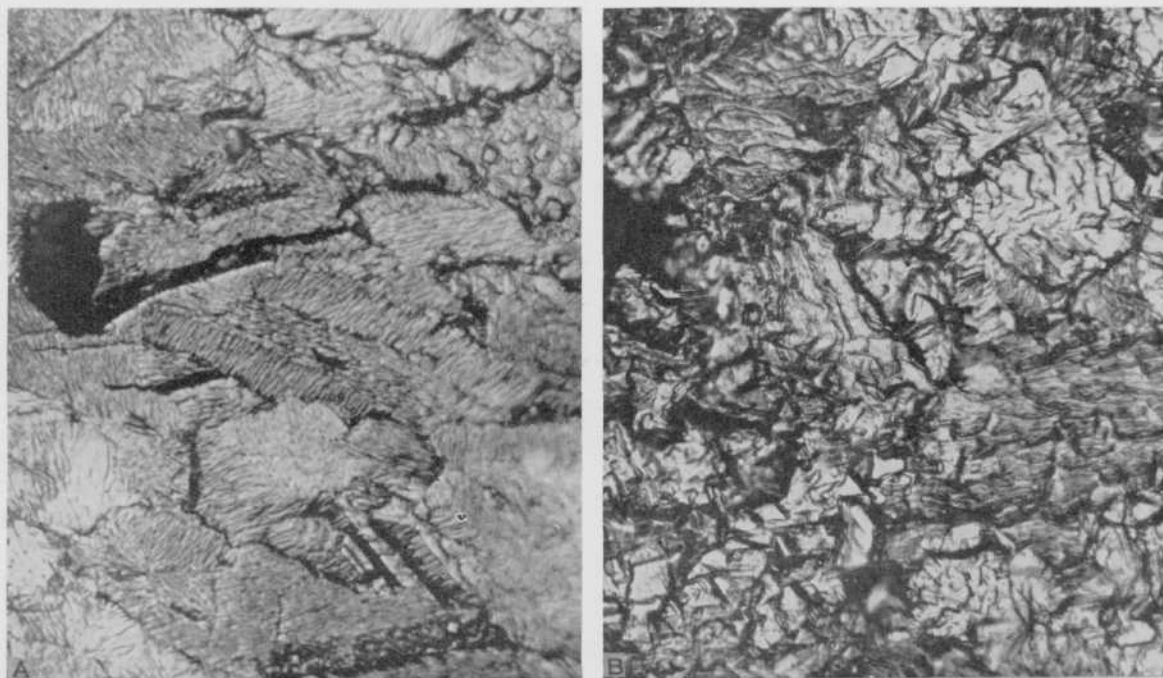


FIGURE 27. Effect of testing conditions on structure of copper initially as annealed.

Longitudinal sections etched in 3.5 parts glacial acetic acid and 4.5 parts nitric acid (conc.), and 2 parts absolute alcohol, $\times 750$.

	Test		Remarks
	Temperature	Strain rate	
	$^{\circ}F$	%/1,000 hr	
A-----	300	36.4	Structure near axis of specimen 0.10 in. from position of complete fracture. Do.
B-----	300	8.3	

Purification, Purity, and Freezing Points of Twenty-Nine Hydrocarbons of the API-Standard and API-NBS Series¹

By Anton J. Streiff,^{2,3} Laurel F. Soule,² Charlotte M. Kennedy,² M. Elizabeth Janes,^{2,3} Vincent A. Sedlak,² Charles B. Willingham,⁴ and Frederick D. Rossini³

This report describes the purification and determination of freezing points and purity of the following 29 hydrocarbons of the API-Standard and API-NBS series: 2,2,4,6,6-pentamethylheptane; 1,1,2-trimethylcyclopropane; *cis*-2-hexene; *cis*-3-hexene; 2-methyl-1-pentene; 4-methyl-1-pentene; 3-methyl-*trans*-2-pentene; 4-methyl-*cis*-2-pentene; 4-methyl-*trans*-2-pentene; 4,4-dimethyl-1-pentene; 4,4-dimethyl-*trans*-2-pentene; 2,3,3-trimethyl-1-butene; *trans*-4-octene; 1-nonene; 1-decene; 1-undecene; 1,3-butadiene; 1,2-pentadiene; 1, *cis*-3-pentadiene; 1, *trans*-3-pentadiene; 1,4-pentadiene; 2,3-pentadiene; 2-methyl-1,3-butadiene (isoprene); 1,5-hexadiene; 2,3-dimethyl-1,3-butadiene; 4-ethenyl-1-cyclohexene (4-vinyl-1-cyclohexene); *cis*-decahydronaphthalene; *trans*-decahydronaphthalene; 2,3-dihydroindene (indan).

¹ This investigation was performed at the National Bureau of Standards as part of the work of the American Petroleum Institute Research Project 6 on the Analysis, Purification, and Properties of Hydrocarbons.

² Research Associate on the American Petroleum Institute Research Project 6.

³ Present address: Carnegie Institute of Technology, Pittsburgh, Pa.

⁴ Present address: Mellon Institute of Industrial Research, Pittsburgh, Pa.